GCM Aerosols

Aerosol Working Group Meeting

September 17-19, 2007

Madison, WI

Andrew A. Lacis

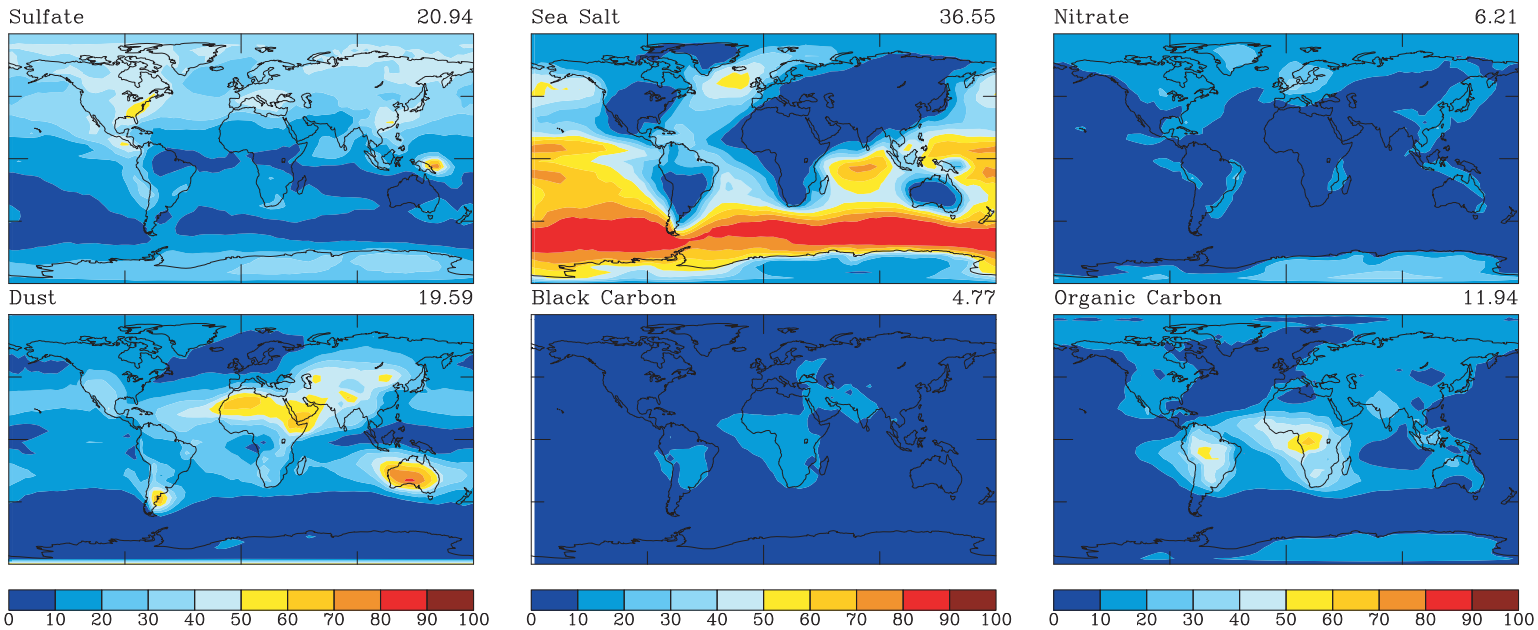

Figure 3. Fractional distribution of principal species (per cent) of GISS annual-mean aerosol climatology

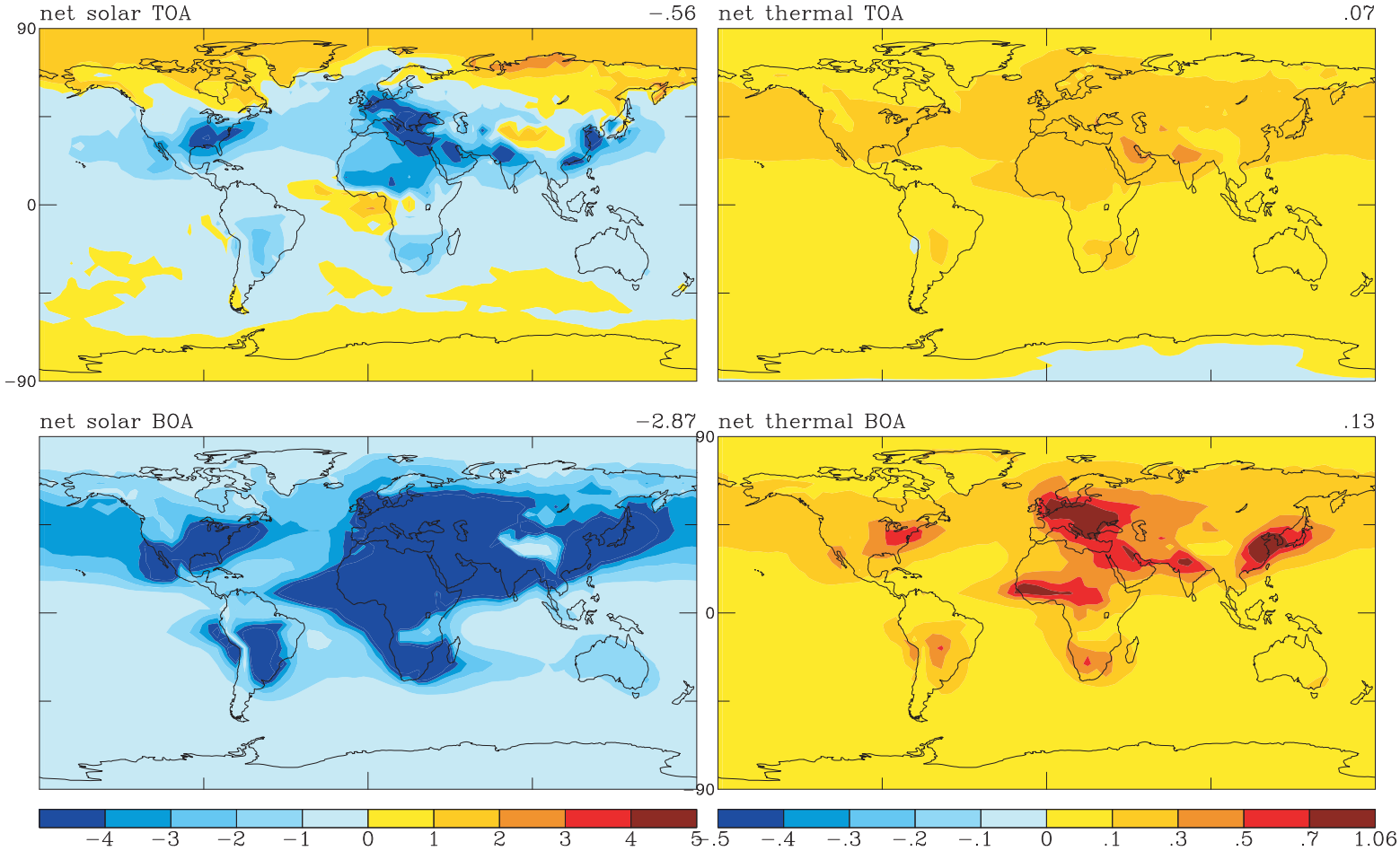

SW and LW aerosol radiative forcings at TOA and BOA for current climate relative to pre-industrial conditions.

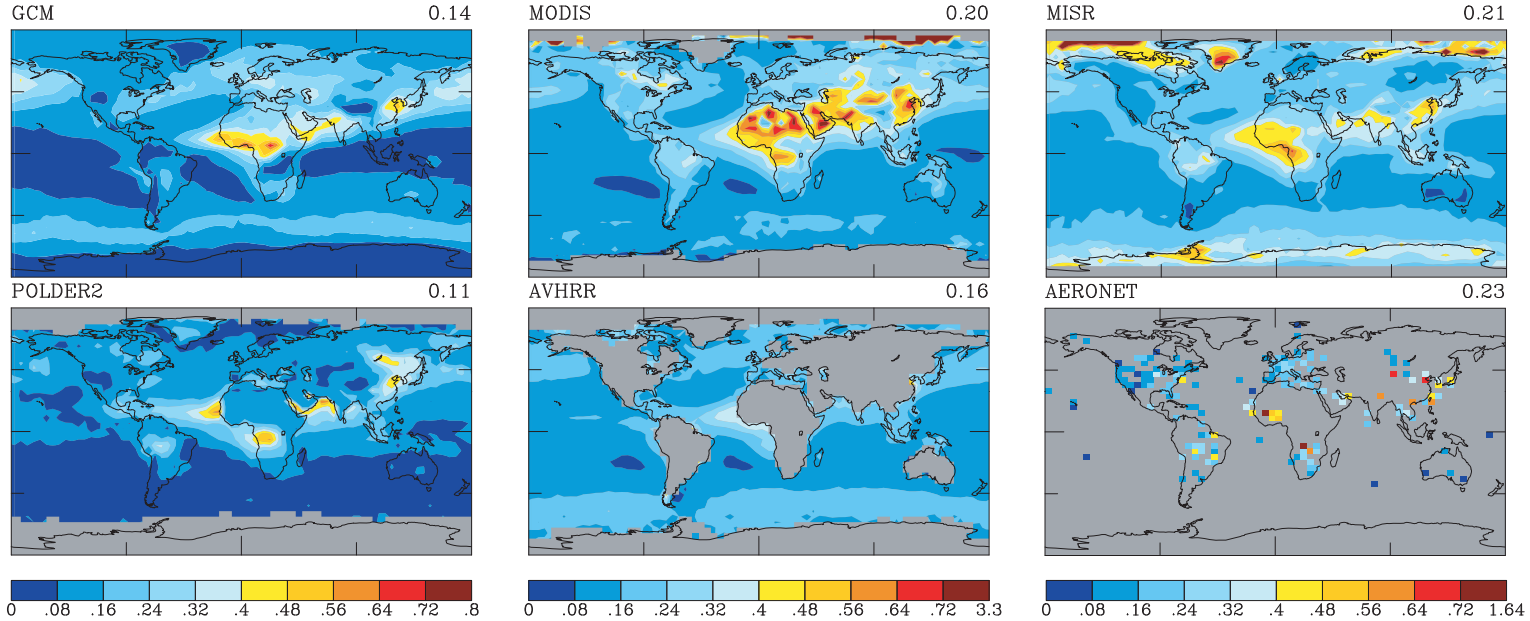

Figure 1. Qualitative agreement for the overall annual mean aerosol optical depth at 0.55 μm compiled from different datasets. Numbers at top right corner represent the area weighted global means.

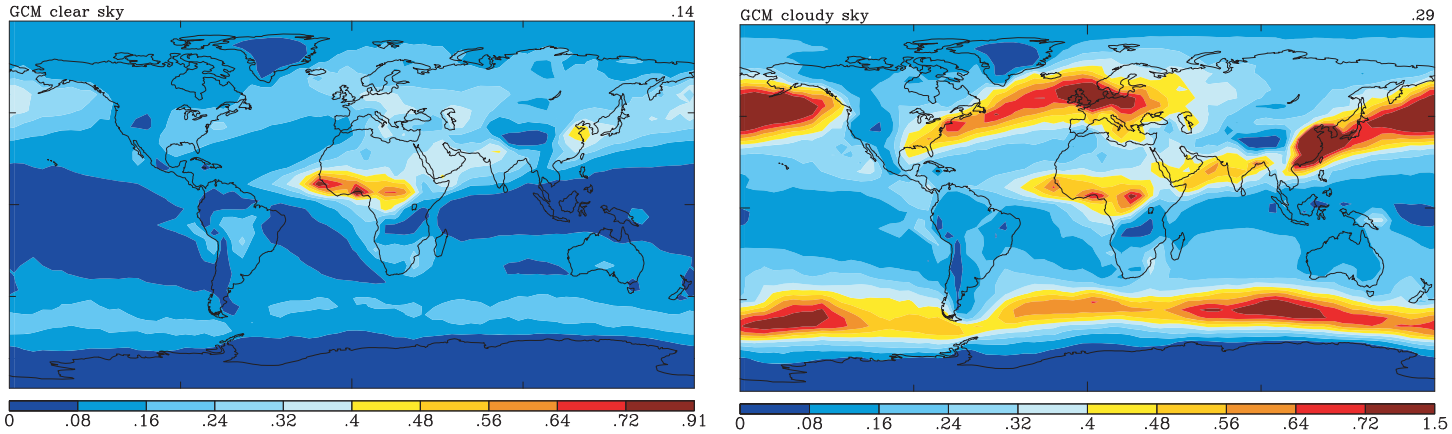

Figure 15. Annual mean GCM aerosol optical depth for clear-sky (left) and cloudy-sky (right) conditions. Numbers in the upper right corner of the plots are area weighted global mean optical depths at 0.55μm.

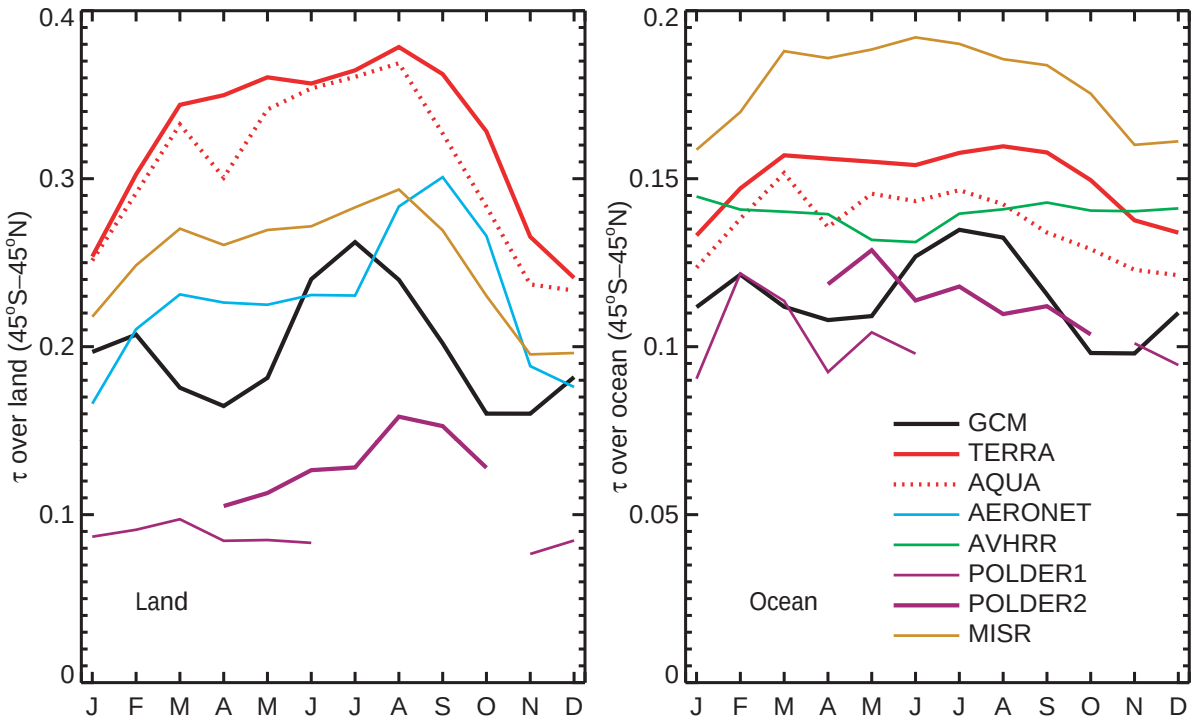

Figure 4. Seasonal dependence of area weighted overall monthly mean aerosol optical depth from different data sources. Data over ocean (left panel) and over land (right panel) have been averaged over 45° S – 45° N and over available data of the respective instruments.

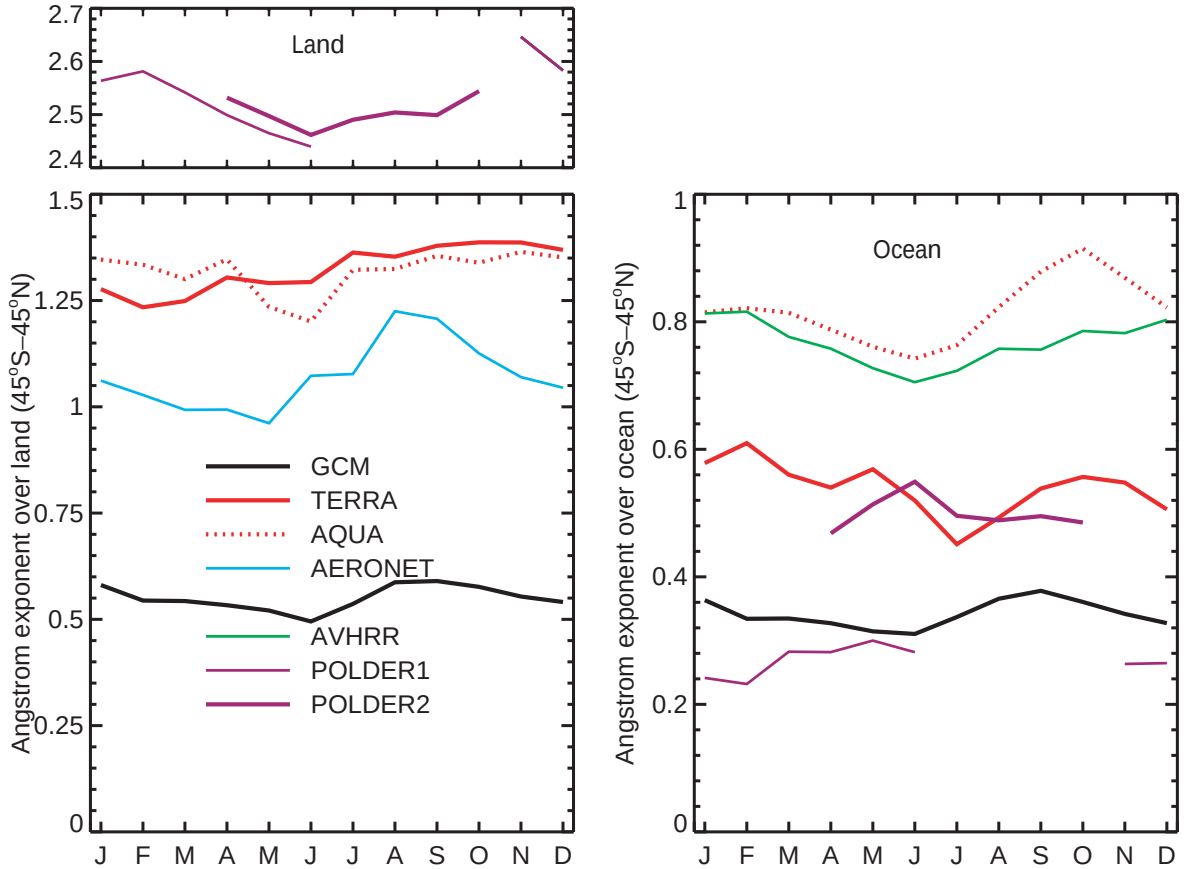

Figure 5. Same as Fig. 4, but the averaged data are for the Ångström exponent.

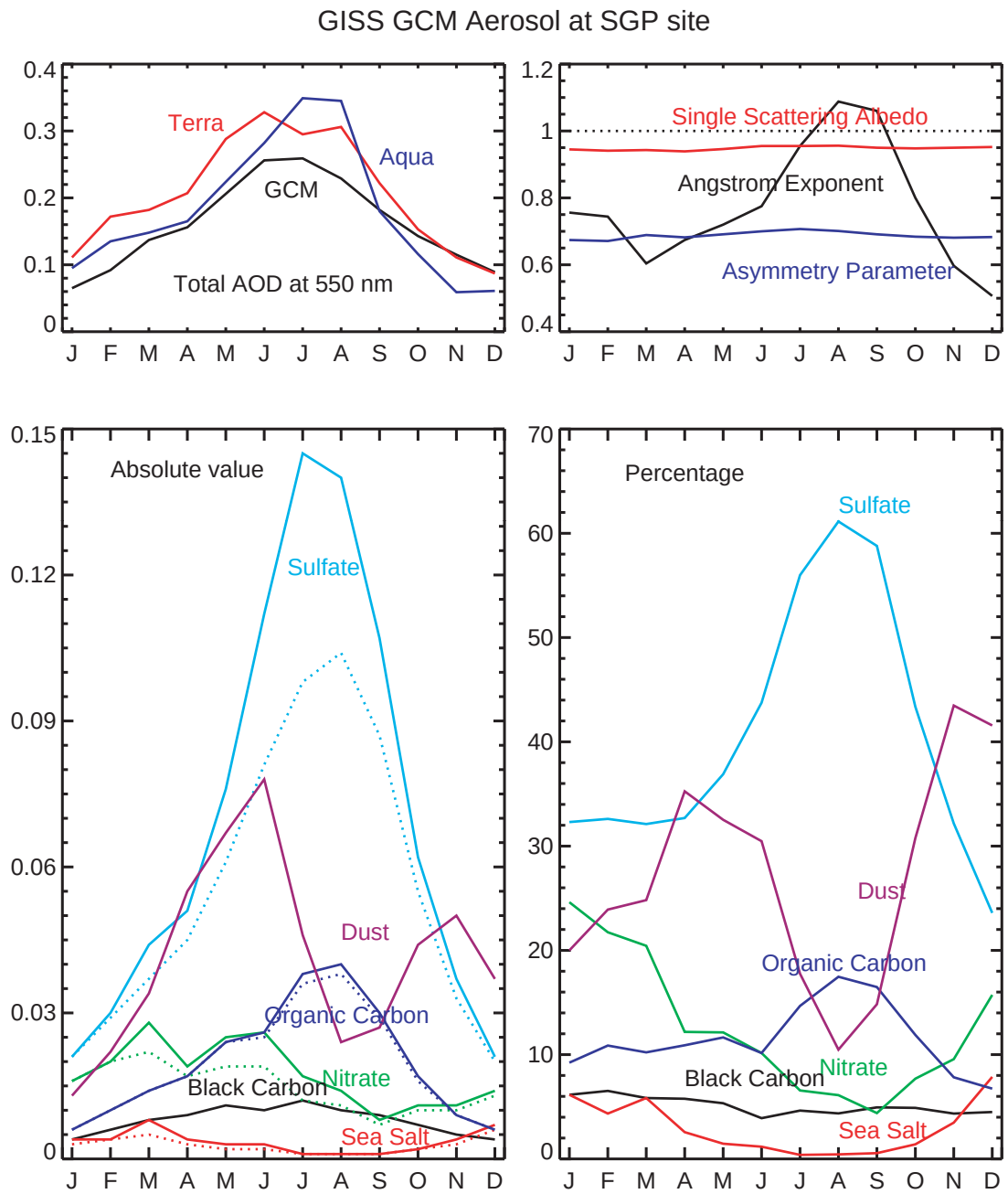
GISS GCM Aerosol at SGP site
Terra
Aqua
GCM
Total AOD at 550 nm
Single Scattering Albedo
Angstrom Exponent
Asymmetry Parameter
Absolute value
Sulfate
Dust
Organic Carbon
Nitrate
Black Carbon
Sea Salt
Percentage
Sulfate
Dust
Organic Carbon
Nitrate
Black Carbon
Sea Salt
J F M A M J J A S O N D

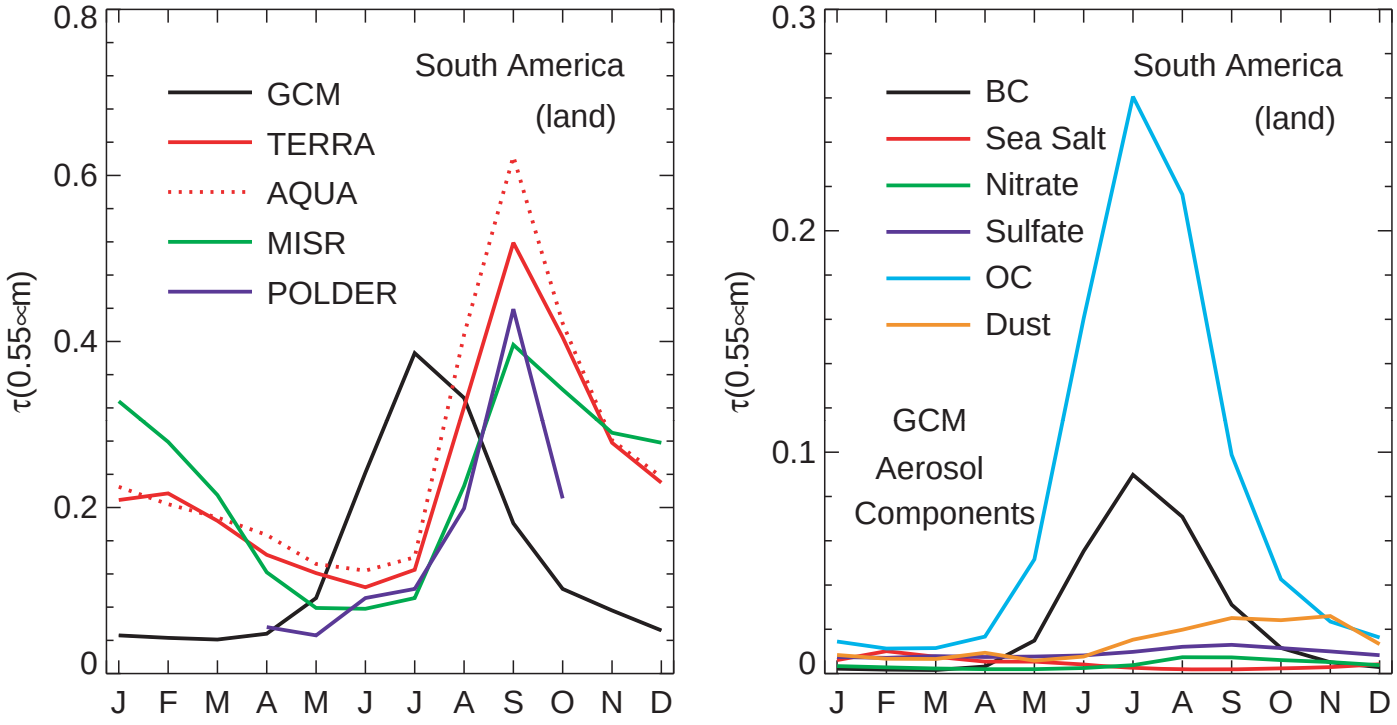

Seasonal variability phase error of GCM aerosol (over South America) associated with organic carbon and black carbon source specification.

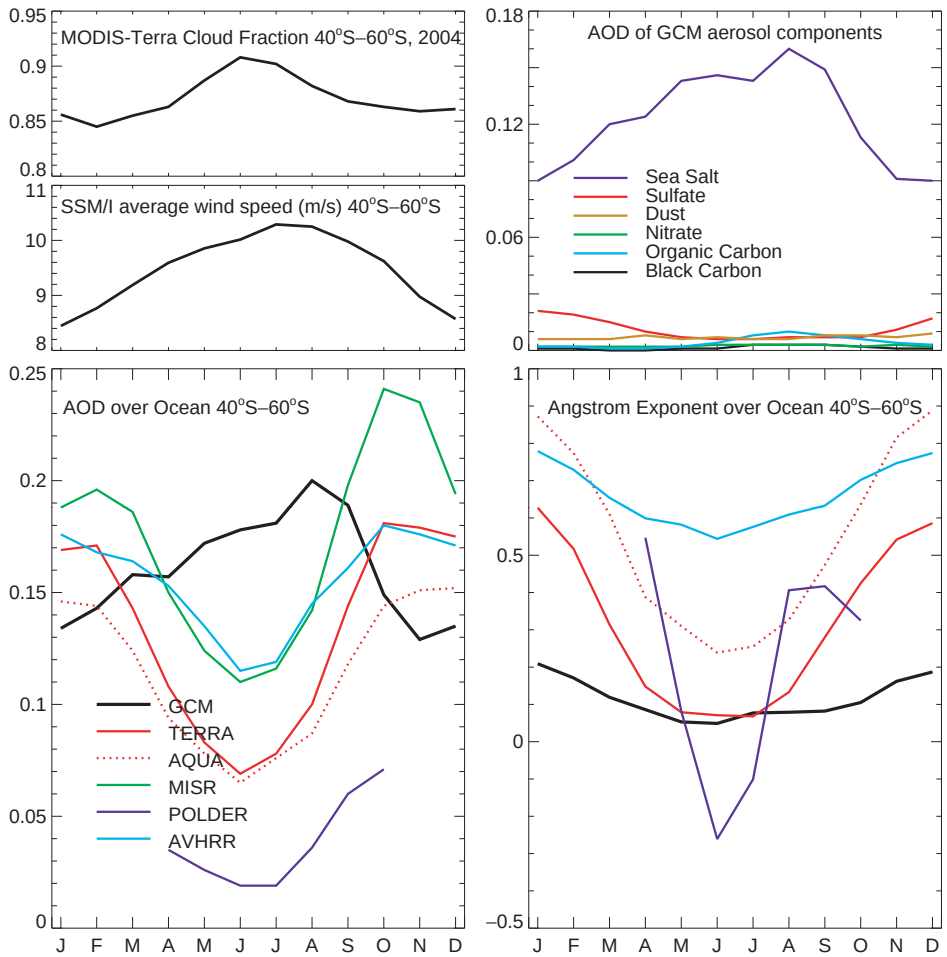

Seasonal phase mismatch of aerosol optical depth variability between GCM (sea salt) and satellite observations.

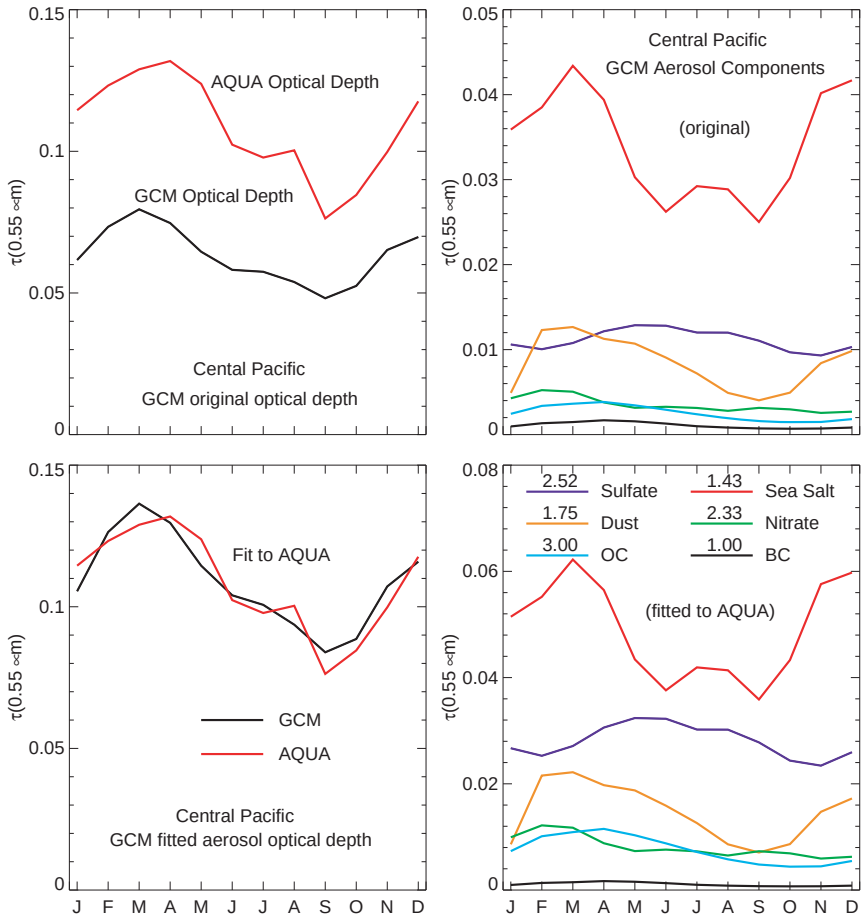

Adjustment of GCM aerosol component optical depths (in Central Pacific) to match seasonal variability of AQUA measurements.

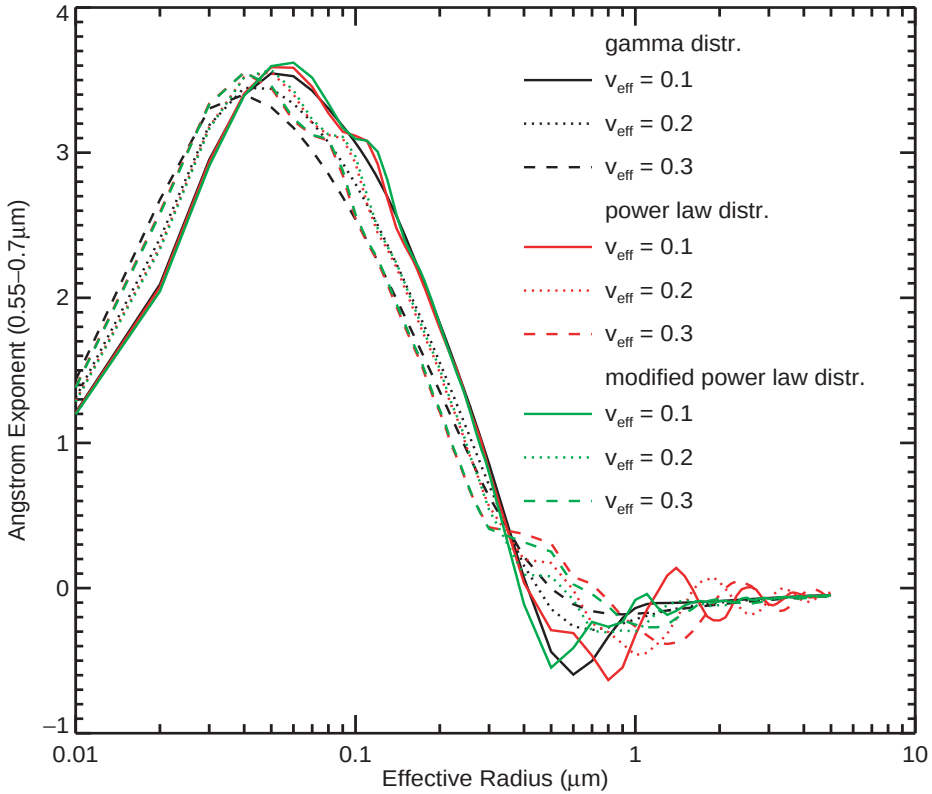

Figure 6. Ångström exponent dependence on aerosol size, computed for nominal refractive index of 1.5 + 0.003 *i*, for spectral interval 0.55 to 0.7 μm versus effective radius for different size distributions.

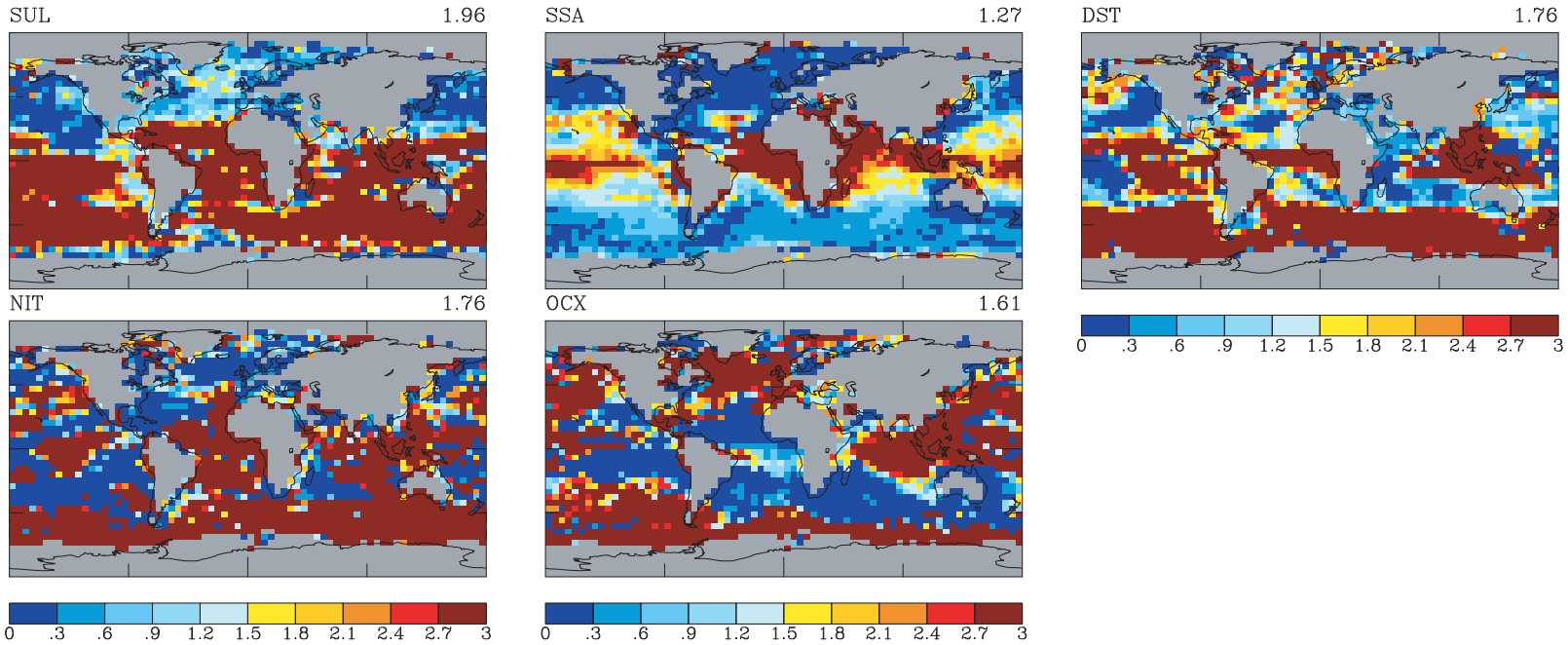

Adjustment of GCM aerosol component optical depths at each grid box (size kept fixed) to match optical depth and seasonal variability of AQUA observations.

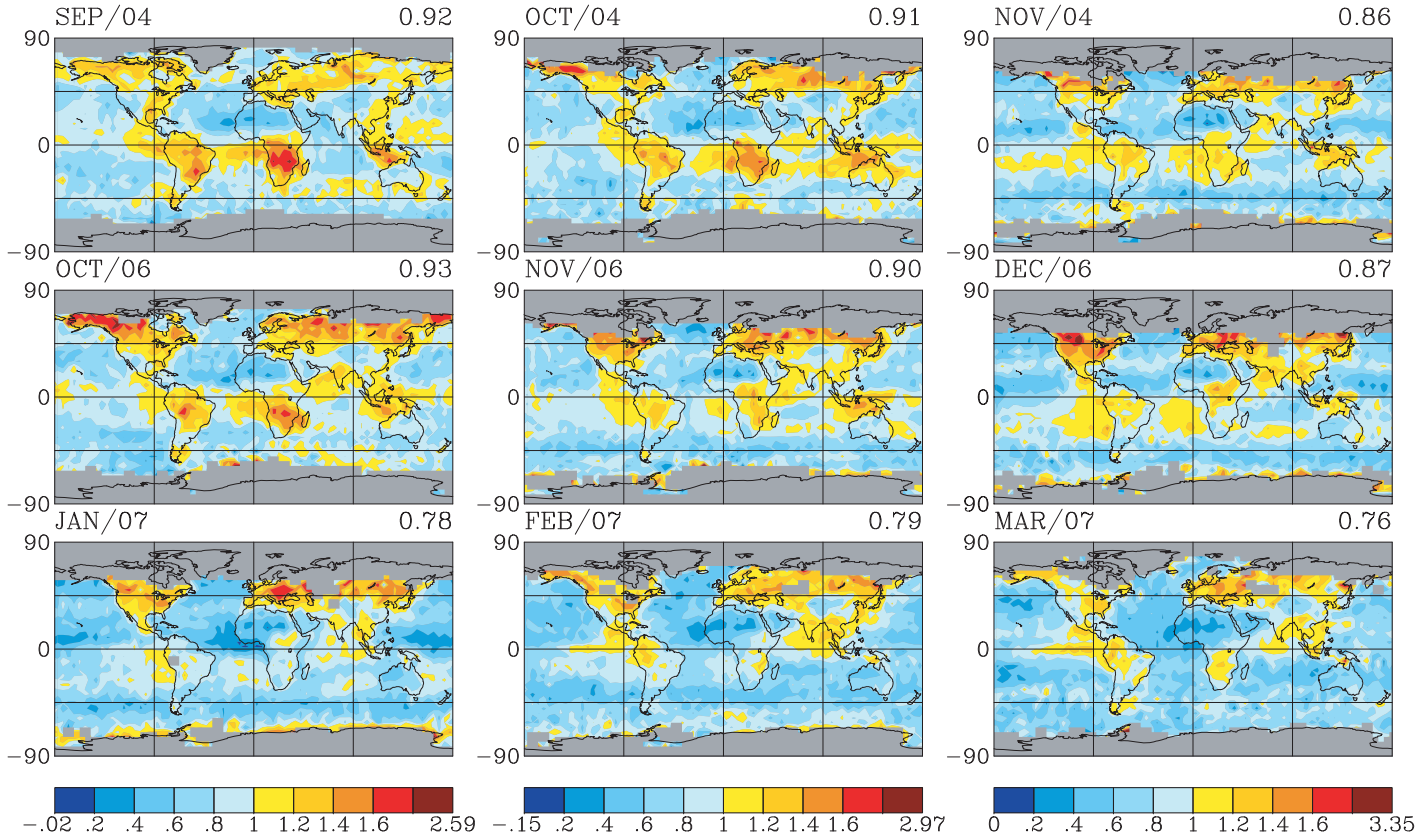

MISR Angstrom Exponent

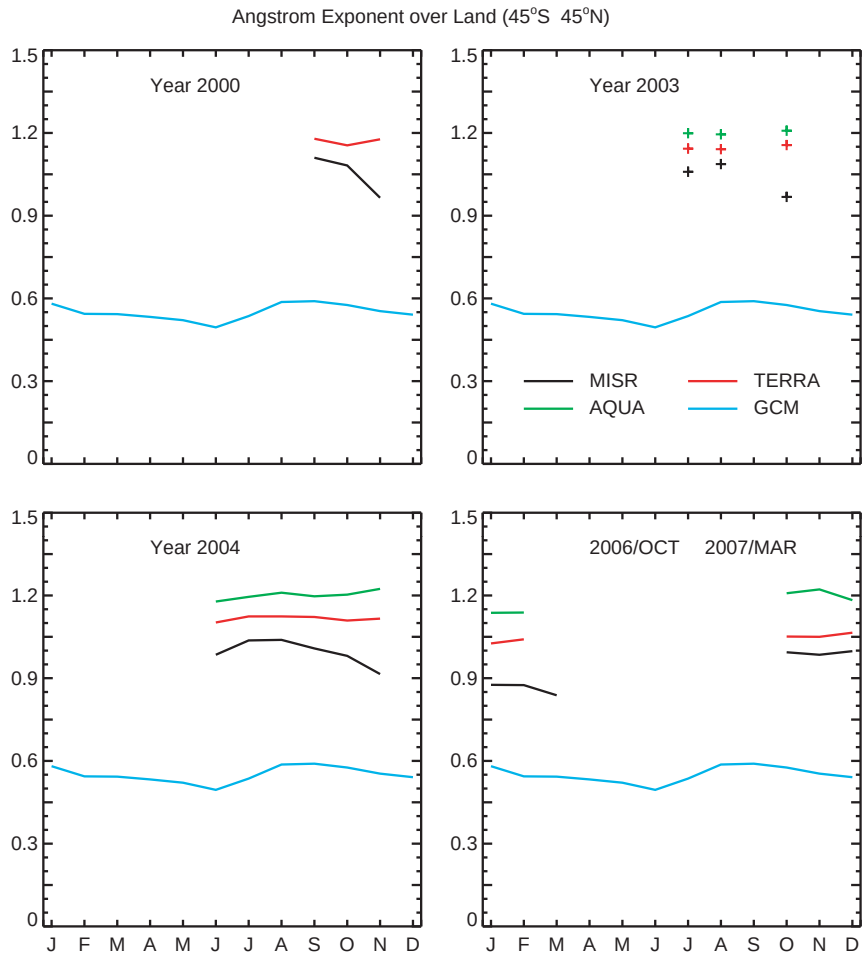
Angstrom Exponent over Land (45°S 45°N)
Year 2000
Year 2003
Year 2004
2006/OCT 2007/MAR
MISR
TERRA
AQUA
GCM
1.5
1.2
0.9
0.6
0.3
0
J F M A M J J A S O N D

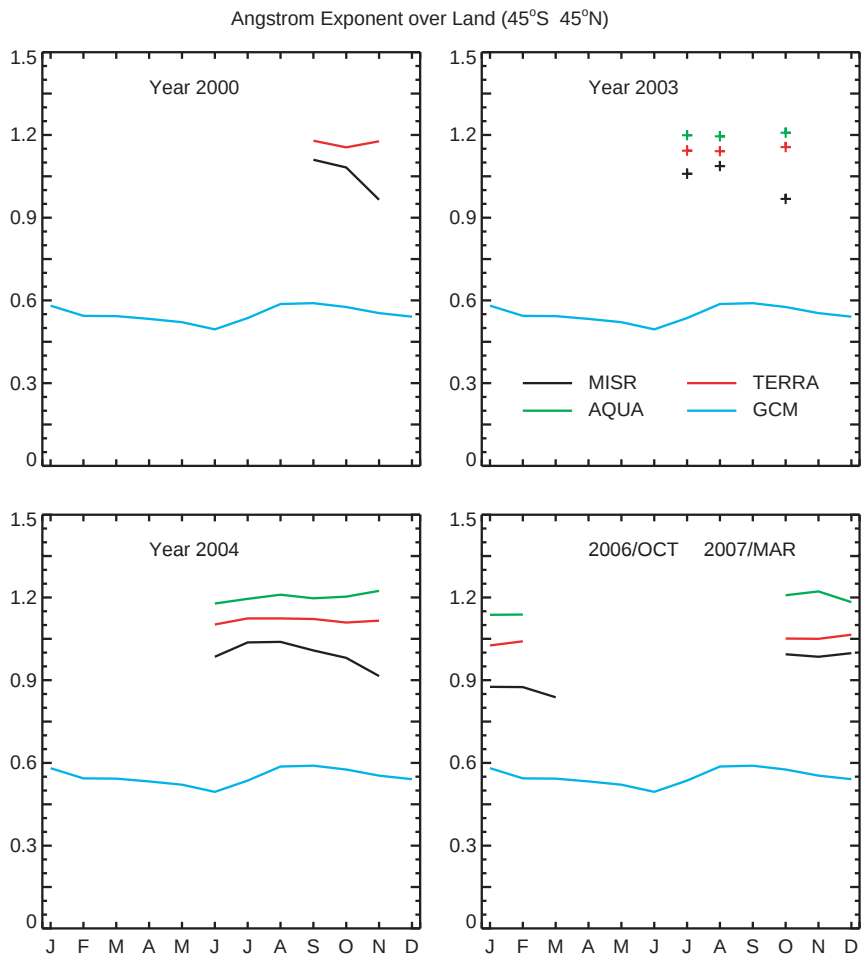
Angstrom Exponent over Land (45°S 45°N)
Year 2000
Year 2003
Year 2004
2006/OCT 2007/MAR
MISR
TERRA
AQUA
GCM
1.5
1.2
0.9
0.6
0.3
0
J F M A M J J A S O N D

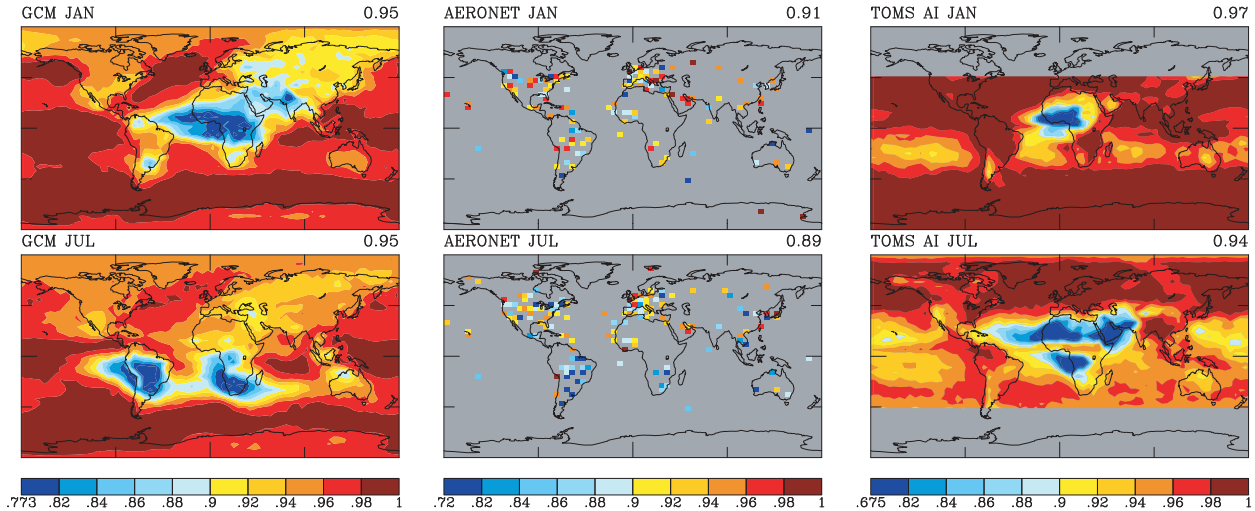

Figure 14. January and July monthly- mean single scattering albedo for the GISS ModelE aerosol climatology for 1990 (left panels). TOMS Aerosol Index (AI) (right panels) has been re-scaled as (1 Š 0.1×AI) to roughly resemble the GCM single scattering albedo. Aerosol single scattering albedo measured locally at AERONET network sites is shown in the center panels. Numbers appearing in the upper right corners are area weighted global mean values.

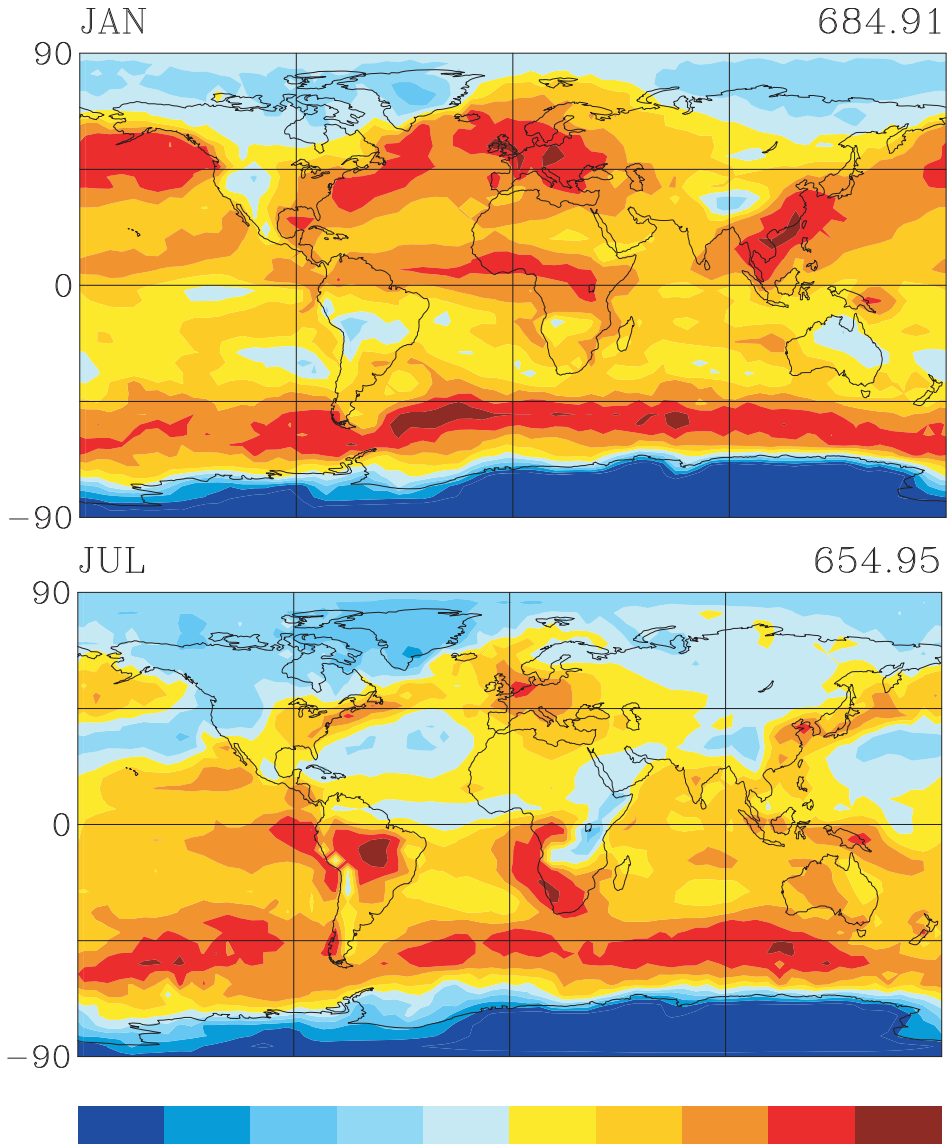

Seasonal height variability of GCM aerosols expressed as mean pressure (mb).

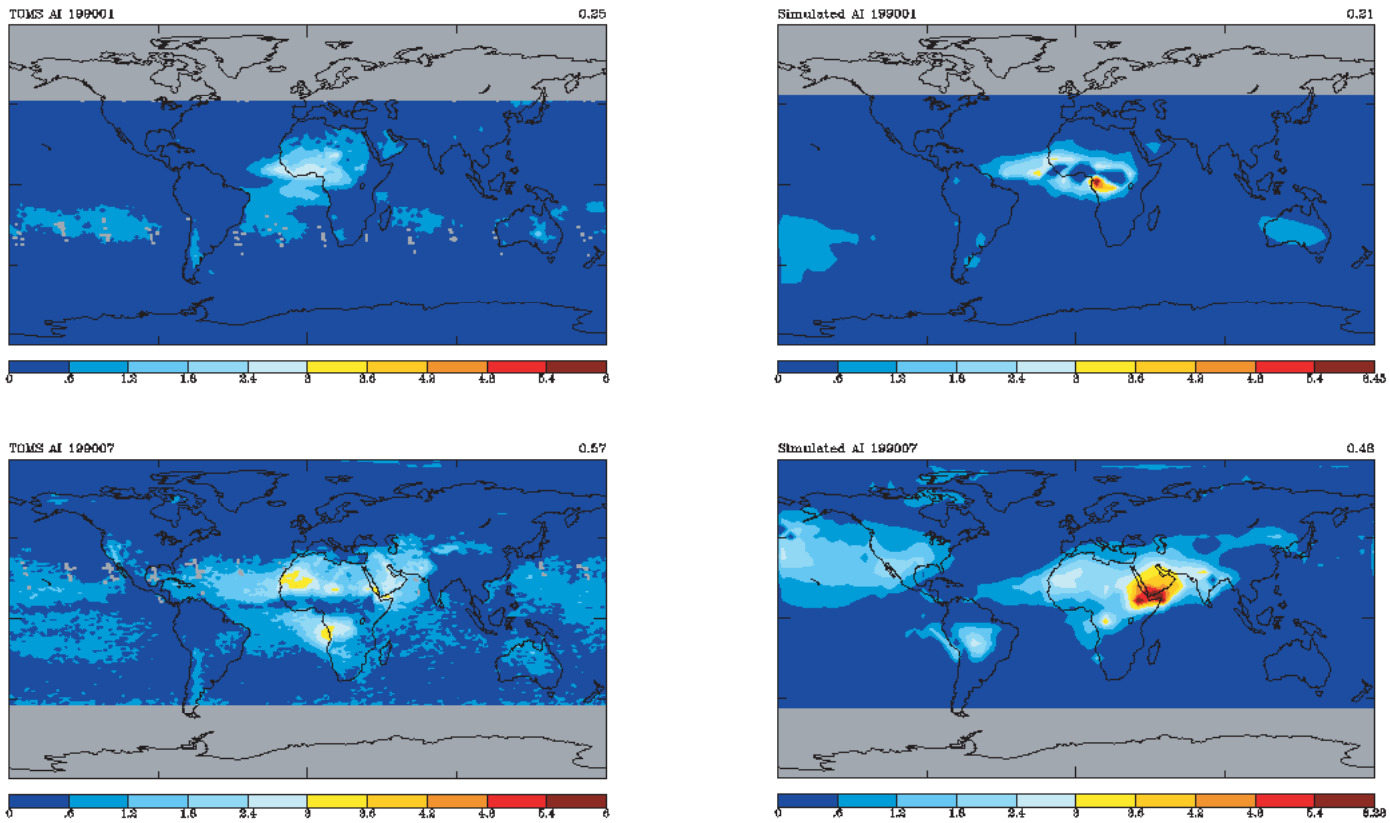

Sample TOMS Aerosol Index (left), and preliminary GCM simulated TOMS AI (right).

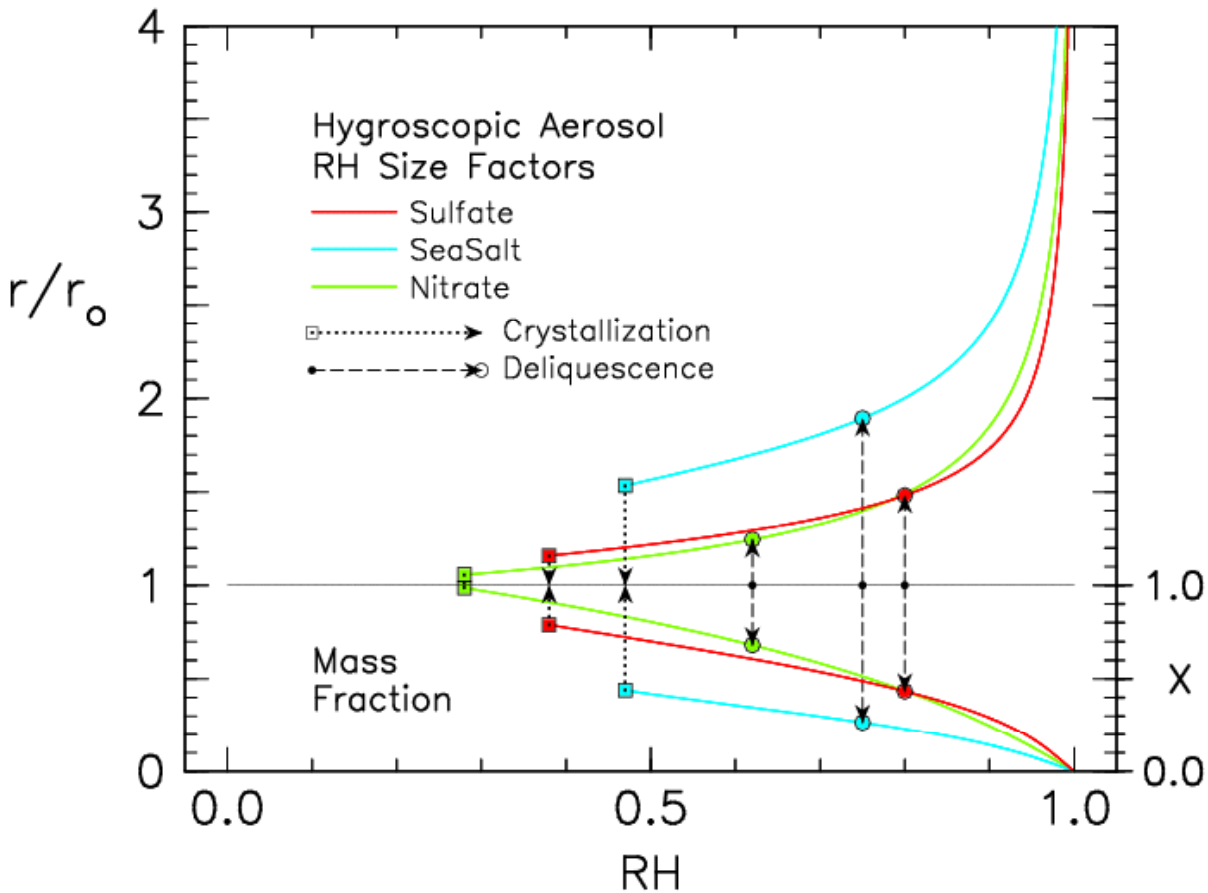

Hygroscopic aerosol size and (dry) mass fraction as a function of relative humidity relative humidity. The size, density, and refractive index of hygroscopic aerosols follows a hysteresis loop according to laboratory measurements by Tang and Munkelwitz [1991, 1994, 1996]. With rising relative humidity, a dry aerosol rapidly becomes a solute particle at the deliquescence point (filled circles), dropping from the equilibrium curve as RH decreases below the crystallization point (filled squares).

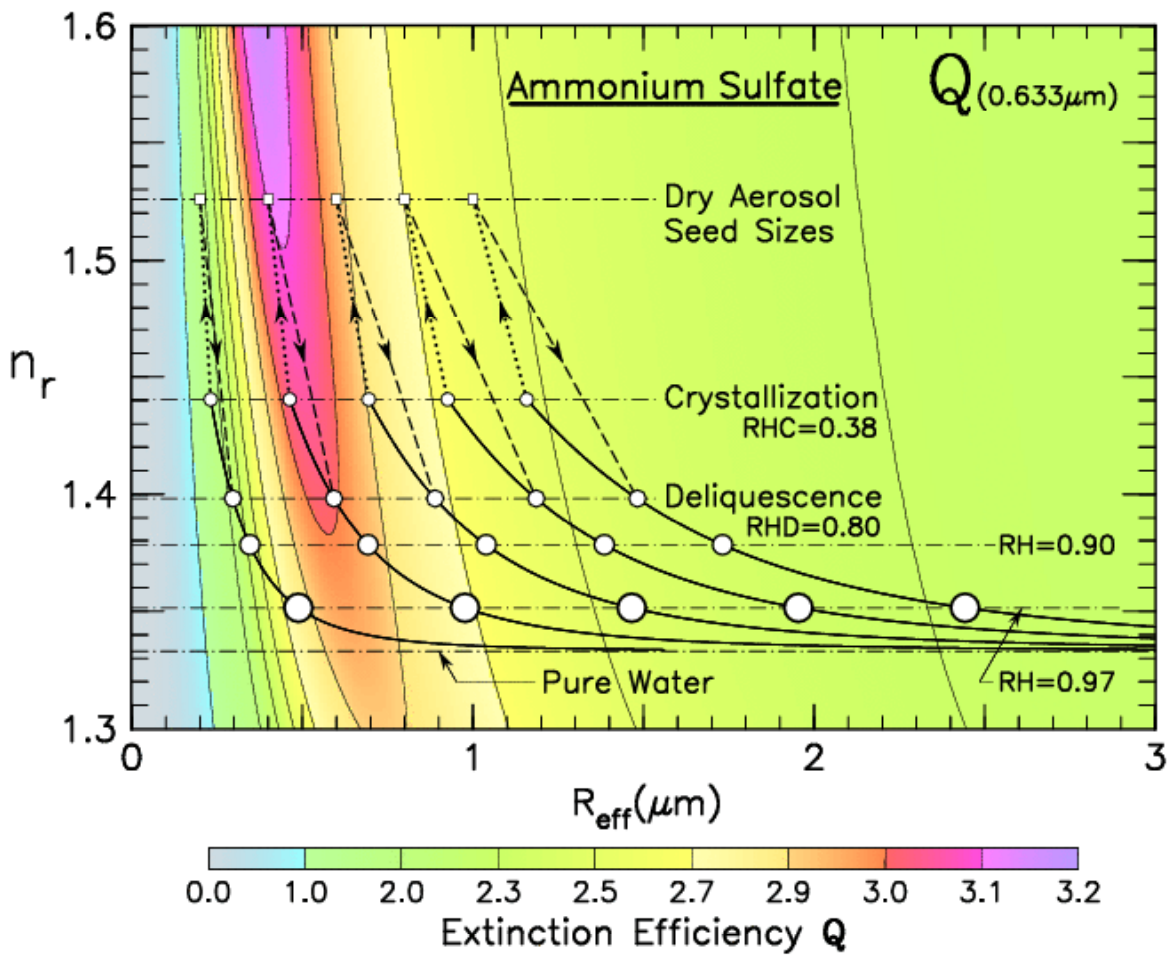

Relative humidity constrained tracks, according to laboratory measurements by Tang and Munkelwitz [1991, 1994, 1996], in Mie scattering extinction efficiency parameter map for selected dry sulfate seed sizes. White squares depict selected dry aerosol (200 to 1000 nm) seed sizes. Dashed arrow lines show deliquescence transitions at RHD=0.80. Dotted arrow lines depict crystallization points at RHC=0.38. White circles designate relative increase in solute aerosol size with increasing relative humidity.

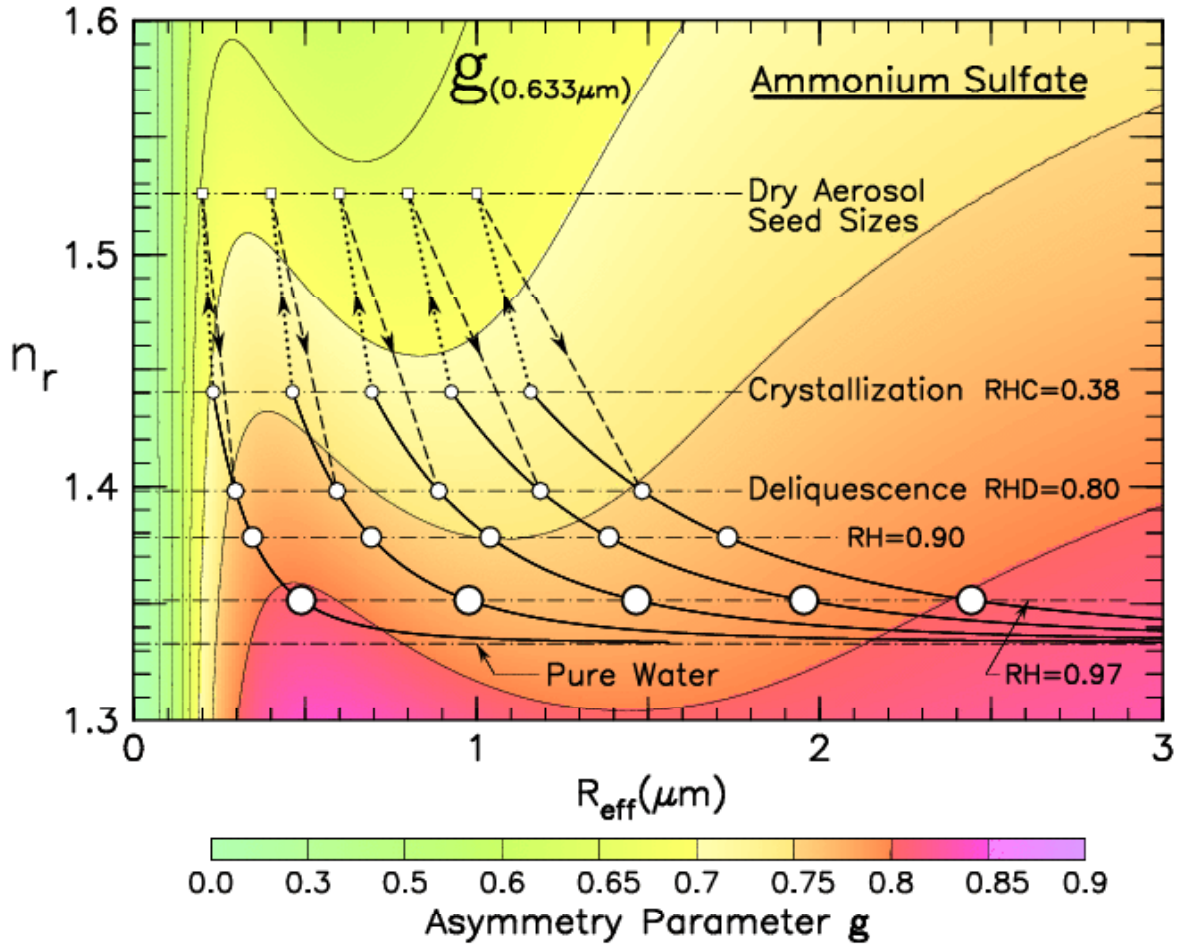

Relative humidity constrained tracks, according to laboratory measurements by Tang and Munkelwitz [1991, 1994, 1996], in Mie scattering asymmetry parameter map for selected dry sulfate seed sizes. White squares depict selected dry aerosol (200 to 1000 nm) seed sizes. Dashed arrow lines show deliquescence transitions at RHD=0.80. Dotted arrow lines depict crystallization points at RHC=0.38. White circles designate relative increase in solute aerosol size with increasing relative humidity.

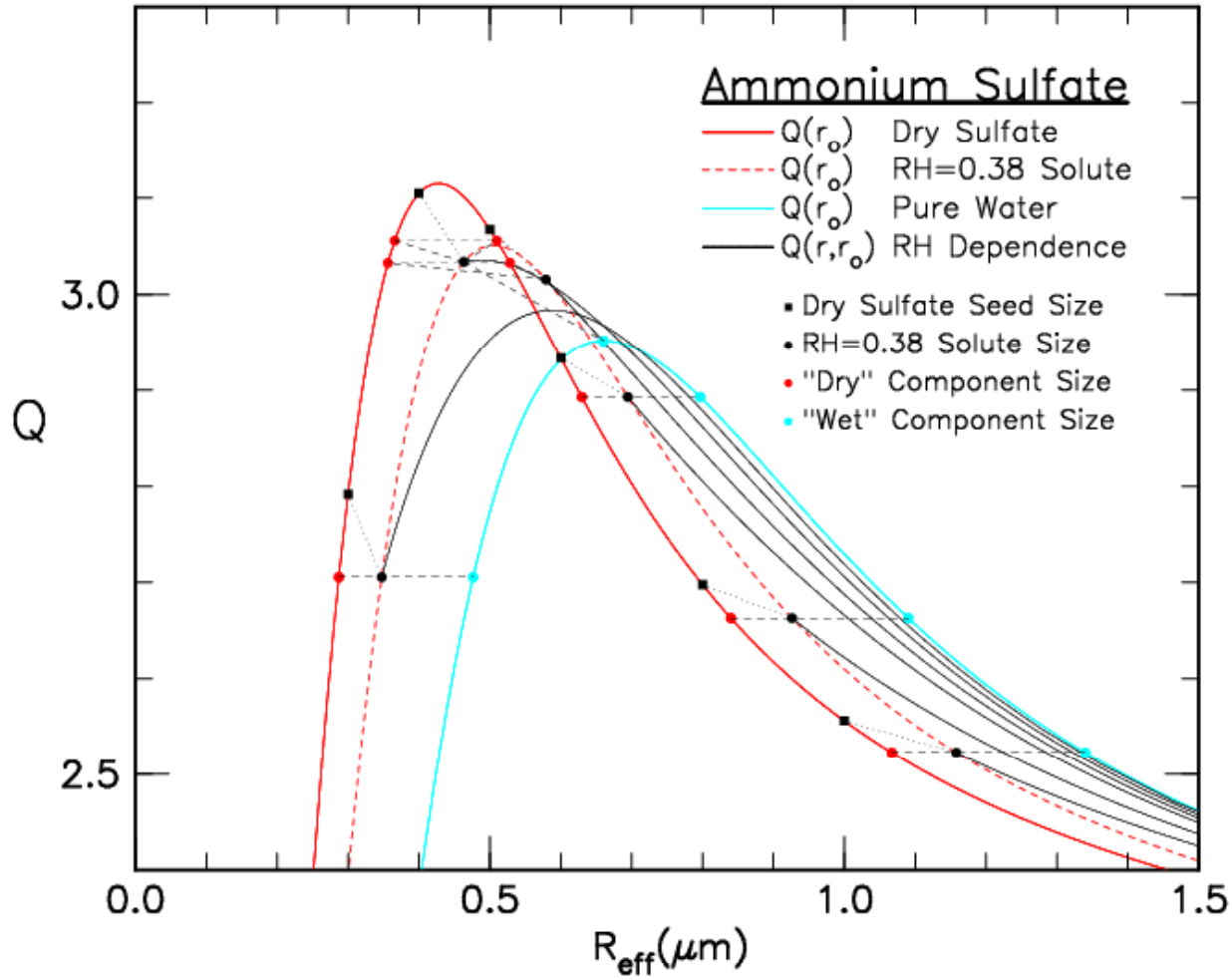

Representation of solute particle radiative parameters (extinction efficiency and asymmetry parameter) as a weighted average of dry aerosol (solid red) and pure water (blue) aerosol properties. The dashed red line depicts the RH=0.38 crystallization point for sulfate aerosols. The black lines depict equilibrium RH dependent Q(R) for specified dry aerosol seed sizes. Since Q is the same (along horizontal dashed lines), the asymmetry parameter of the solute aerosol can be precisely matched as a weighted average of the pure dry and pure water aerosol values of the appropriate sizes, as indicated.

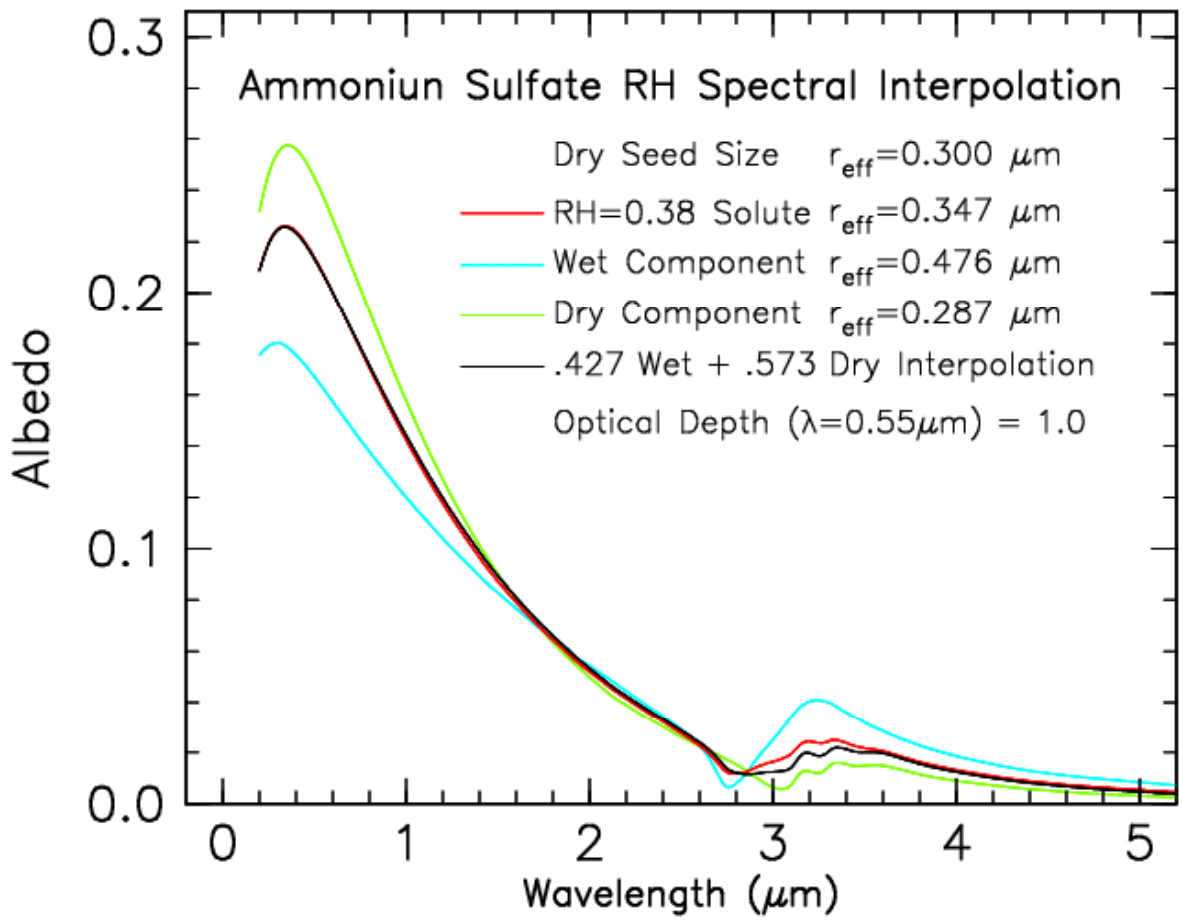

Spectral validation of the pure dry/pure water (PDPW) weighted average representation of solute aerosol radiative properties. The (reference) red curve utilizes Mie scattering parameters computed for the appropriate solute spectral refractive index at RH=0.38. The black line depicts the spectral albedo computed with the averaged PDPW radiative parameters. Thus, the radiative properties of a 300 nm dry sulfate aerosol, which becomes a 347 nm solute particle at RH=0.38, can be accurately represented as the weighted average of a pure dry 287 nm particle and a 476 nm pure water aerosol.